Geoderma 187–188 (2012) 31–40

Contents lists available at SciVerse ScienceDirect

Geoderma

journal homepage: www.elsevier.com/locate/geoderma

Assessing the role of the pore solution concentration on horizontal deformations in an unsaturated soil specimen during drying

Majdi Abou Najm [a,b,c,*], Julie Jesiek [d], Rabi H. Mohtar [d,e], Pietro Lura [f,g], Gaurav Sant [h,i]

[a] American University of Beirut, Department of Civil & Environmental Engineering, Beirut, Lebanon
[b] Oregon State University, Biological and Ecological Engineering, Corvallis, OR, USA
[c] Massachusetts Institute of Technology, Department of Civil and Environmental Engineering, Cambridge, MA, USA
[d] Department of Agricultural and Biological Engineering, 225 South University Street, West Lafayette, IN 47907, USA
[e] Qatar Environment and Energy Research institute, Qatar Foundation, Doha, Qatar
[f] Laboratory for Concrete/Construction Chemistry, EMPA, Swiss Federal Laboratories for Materials Science and Technology, Überlandstrasse 129, CH-8600 Dübendorf, Switzerland
[g] Institute for Building Materials (IfB), ETH Zurich, Schafmattstrasse 6, 8093 Zürich, Switzerland
[h] Department of Civil and Environmental Engineering, University of California, Los Angeles, CA 90095, USA
[i] California Nanosystems Institute, University of California, Los Angeles, CA 90095, USA

ARTICLE INFO

Article history:
Received 28 August 2011
Received in revised form 5 April 2012
Accepted 14 April 2012
Available online 22 May 2012

Keywords:
Stress-Strain
Restrained Ring Method
Drying
Volume Change
Salinity
Shrinkage-Swelling

ABSTRACT

Volume changes occurring in soil–water systems are the result of multi-scale interactions that affect several processes in the soil–water continuum. For example, the soil's shrinkage/swelling properties result in horizontal and vertical deformations at the soil specimen scale, and lead to cracking which is often responsible for producing preferential flow paths that impact the hydrologic response at the plot and field scales. In spite of their significance, a complete understanding of soils' deformations and their corresponding impact on volume change behavior continues to be a major challenge. This paper presents an approach to quantify and interpret the role of the pore solution concentration on horizontal deformations of unsaturated soils. Specifically, a restrained ring method (RRM) is integrated with digital image correlation (DIC) techniques to relate the internal soil stress (caused due to drying) to the shrinkage strain (deformation) that develops in the soil specimen. The experimental results are described in the context of the theory of drying while explicitly considering the effect of changes in the properties of the pore solution (i.e., surface tension, viscosity and density) induced by the addition of a binary salt (NaCl). The experimental results conform to fundamental expectations and thereby this approach facilitates a better understanding of volume changes in unsaturated soils exposed to saline environments.

1. Introduction and background

Several interconnected processes govern volume changes in unsaturated soils. In the absence of a complete theoretical and experimental framework, an explanation of this multi-scale process has been lacking. This situation has been further exacerbated by disconnected observations of volume changes in soils at the laboratory and field scales (Abou Najm, 2009; Chertkov, 2008a, b; Taboada et al., 2008). Depending on scale, volume changes may manifest as: (1) cracks and fissures (Abou Najm et al., 2010; Bogner et al., 2008; Kung et al., 2000; Williams et al., 2003) at the field scales, (2) bulk macroscopic deformations of the soil specimen at the laboratory scale (shrinkage, swelling, consolidation), and (3) soil–water interaction at the individual particle and aggregate scales resulting in soil structure changes (Or and Tuller, 1999).

Current methods to assess volume change at the bulk macroscopic scale include the soil mechanics approach which typically considers volume change as a function of the externally applied (overburden) pressure as relevant in geotechnical engineering applications. Thus, volume change is described as strain that results from a change in the effective stress (internal and external) level (Fredlund and Morgenstern, 1977; Fredlund and Rahardjo, 1993; Khalili et al., 2004; Matyas and Radhakrishna, 1968; Murray, 2002). Another approach involves monitoring the change in the bulk volume of soil cores as function of the pore pressure or moisture content assuming the soil is in equilibrium with its environment. Thus, volume changes (i.e., shrinkage or swelling) are related to the soil's moisture content through the development of shrinkage (Braudeau et al., 2004; Chertkov, 2007; Cornelis et al., 2006; Giraldez et al., 1983; McGarry and Malafant, 1987; Olsen and Haugen, 1998; Peng et al., 2006) and swelling (Braudeau and Mohtar, 2006) curves, as well as the soil–water characteristic curve (Baumgartl and Koeck, 2004; Chertkov,

* Corresponding author at: American University of Beirut, Department of Civil and Environmental Engineering, Beirut, Lebanon. Tel.: +961 71 567 771; Fax: +961 1 744 462.
E-mail addresses: majdian@aub.edu.lb, majdi@engr.orst.edu, majdi@mit.edu (M. Abou Najm), rmohtar@qf.org.qa (R.H. Mohtar), pietro.lura@empa.ch (P. Lura), gsant@ucla.edu (G. Sant).

0016-7061/$ – see front matter © 2012 Elsevier B.V. All rights reserved.
doi:10.1016/j.geoderma.2012.04.009

2010; Delage, 2007; Fityus and Buzzi, 2009; Giraldez and Sposito, 1983). A third approach describes the shrinkage of a porous medium (e.g., soil, concrete, etc.) as a drying (moisture loss) problem, wherein a balance between evaporation and moisture transport towards an exposed surface dictates volume changes; by considering the existence of spatial moisture gradients in the material (Coussy et al., 1998; Roper, 1966; Scherer, 1990).

However, and in spite of multiple approaches, it is yet difficult to describe: (1) the role of soil structure, texture and pore-fluid properties, (2) hysteresis observed between shrinkage and swelling and (3) the effects of the "source-of-stress" such as compaction or overburden pressures on the overall volumetric response. For example, soils of different textures exhibit different volume change behavior when the pore-fluid properties or drying regime are altered, suggesting an interplay between these parameters (Musielak and Mierzwa, 2009; Péron et al., 2007). This has powerful implications, as soil texture and pore-fluid properties affect the depth, width, spacing, and shape of cracks (the manifestation of volume change at the field-scale) which in turn influence the hydraulic/mechanical properties of the medium (Dane and Klute, 1977; Jozefaciuk et al., 2006; Lima and Grismer, 1992; McNeal et al., 1966; Musielak and Mierzwa, 2009; Oster and Schroer, 1979; Péron et al., 2007; Sartori et al., 1985; Waller and Wallender, 1993).

This paper assesses the role of fluid-properties and the impact of salt concentration on soil specimen deformations. It describes the results of a series of interconnected experiments which relate the salt (i.e., NaCl) concentration and pore solution properties to the stress and strain developed during drying. The experimental results are interpreted in the context of traditional concepts of drying to describe the macroscopic effects of salinity and pore solution properties on the horizontal deformation of a soil specimen and its impact on the volume change response.

2. Materials and experimental methods

A Chalmers silty-clay loam soil was selected for evaluation in this study. The soil was obtained from the Agronomy Center for Research & Education (ACRE) at Purdue University (Location: Latitude 40°29′38″N and Longitude 86°59′35″W). Several types of analyses were performed on the Chalmers soil. Soil water characteristic curves (SWCC) were obtained for specimens saturated using: (a) deionized (DI) water and (b) 0.60 M (molar) NaCl solution to determine the influence of the solution composition on water retention (Fig. 1a). For each soil, five points on the SWCC were obtained using the pressure plate method at suction values of 10, 33, 100, 500, and 1500 kPa. Assuming $\theta_{1500\ kPa}$ is the residual volumetric water content, the three parameters of the van Genuchten model were derived using the RETC formulation (van Genuchten et al., 1991). In addition, a laser-diffraction based particle size analysis of the soil was performed using water and ultra-sonication to disperse the soil particles. The measured particle size distribution is presented in Fig. 1(b). Ranges of 3.0–5.9 for the COLE index and 4.23–14.11 μm/s for the saturated hydraulic conductivity were reported by the Web Soil Survey of the United States Department of Agriculture (USDA).

To determine the influence of solution salinity on stress and strain development, the Chalmers soil was saturated to ≈36% gravimetric water content using: (1) DI-water, (2) 0.08 mol/kg (M) NaCl solution and (3) 0.60 mol/kg (M) NaCl solution before being dried under laboratory conditions at T = 23 ± 2 °C and RH = 50 ± 10%. The solution concentrations were chosen to correspond to the approximate limits imposed by pure water and typical sea-water (3.5% NaCl by mass). The air-dry soil was sieved using a standard #4 sieve (4.75 mm) and then mixed with the appropriate solution to achieve a gravimetric moisture content of ≈36% by mass. The mixture was then left to stand in a sealed condition for 24 h to equilibrate the specimen. This step ensured a homogenous (uniform) distribution of water through the sample, and accounted for the structural rearrangement of the soil, which may occur due to interactions with the salt solution.

The soil thus prepared was then placed in six layers and compacted uniformly using a 12 cm long stainless steel rod at 100 strikes per layer from a uniform height. Details of the procedure and experimental setup are described elsewhere (Abou Najm et al., 2009). The soil was placed outside the inner instrumented ring, and inside the confining outer ring. Both rings were lightly oiled to prevent adhesion and minimize friction between the ring and the soil specimen. In addition, the mass of the entire setup was recorded continuously from the start of the experiment using an electronic balance interfaced to a personal computer to determine the change in the gravimetric moisture content of the soil sample as a function of the drying time. The specimen was left to dry symmetrically (i.e., from top and bottom) under room conditions (T = 23 ± 2 °C) until cracking occurred. At this time, the experiment was stopped and the soil sample was removed

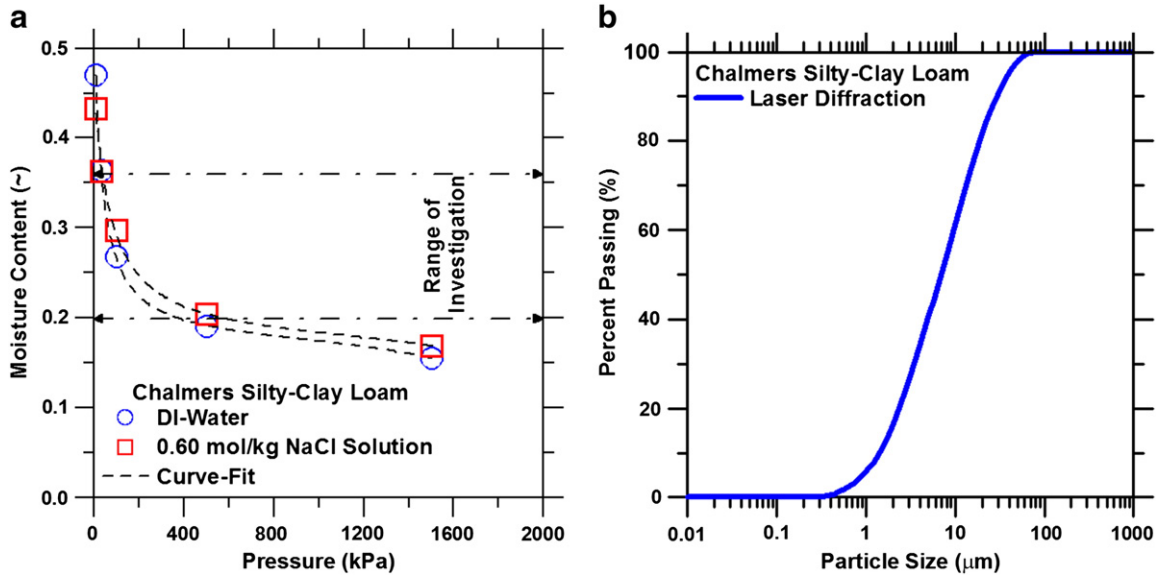

Fig. 1. (a) Soil moisture curve for the Chalmers silty-clay loam as a function of the pressure for soil samples saturated with solutions of varying NaCl concentrations and (b) the particle size distribution of the Chalmers silty-clay loam.

and oven-dried to determine its gravimetric moisture content. This information was used to correlate the magnitude of the internal stress (P_{ISoil}) developed at the interface between the soil and the inner ring to the gravimetric moisture content of the soil specimen. Here, while the restrained ring method (Abou Najm et al., 2009; Hossain and Weiss, 2004) was used to measure restrained shrinkage stresses, a digital camera was placed on top of the soil specimen to determine the magnitude of (shrinkage) strain that developed under restrained conditions.

2.1. Shrinkage calculation using digital image correlation methods

Using a tripod, a digital camera (Canon Powershot 3SIS) was installed above the soil specimen during the restrained ring experiments. The camera utilized was provided with an intervalometer which enabled acquisition of time-lapsed images of the soil specimen at 15 minute intervals. The time-lapsed images were processed in Adobe Photoshop using digital image correlation (DIC) principles to determine the two-dimensional strain developed in the specimen along the *xy* (i.e., horizontal) plane. This was achieved by measuring the change in the area of the soil specimen with increasing moisture loss until cracking occurred, after which image-acquisition was stopped. As such, a maximum delay of 15 min could be expected in the detection of the time of (macroscopic) cracking.

In the first step (Fig. 2) of the analysis, a calibration of image-pixel size was performed as follows: (1) Using the magnetic lasso tool in Adobe Photoshop, the inside perimeter of the outer confining ring was traced and saved as a new layer, (2) for consistency, the selection's color threshold level was set to 128 (in 256 color-mode) so that the selection file can only have pixel values of 0 or 1 and (3) by knowing the inner diameter of the outside ring (R_{OSoil}), the image-pixel area (A_{PIXEL}) was obtained by dividing the total internal area of the specimen by the total number of white pixels. For this setup, with $R_{OSoil} = 5.30$ cm, the average pixel area is around 0.031 mm^2. Knowing the image-pixel area, the second step is to calculate the soil shrinkage area by multiplying the number of pixels inside the soil specimen by the pixel area.

After some drying had occurred, the outer perimeter of the specimen was traced and saved as an independent layer 'shrinkage'. In the presence of discontinuous surface cracks (i.e., cracks that are not continuous from R_{ISoil} to R_{OSoil}), the perimeter of the cracks was also traced and saved as another layer, 'cracks'. As before, the selection's threshold level was set to 128 ensure binary pixel values of 0 or 1. Finally, the number of pixels (N_{SH}) representing the shrinkage area was obtained by subtracting: (selected pixels in 'shrinkage') − (selected pixels in 'cracks'). As such, the shrinking area of the soil specimen (A_{SH}, Eq. (1)) can be calculated for every digital image to quantify the temporal (incremental) change in horizontal shrinkage as the specimen dries. The outer radius of the soil specimen (R_{OSoil}) which varies as the specimen dries and the strain in the *xy* direction (ε_{xy}) can then be calculated as shown in Eqs. (2) and (3):

$$A_{SH} = N_{SH} A_{PIXEL} \tag{1}$$

$$R_{OSoil} = \sqrt{\left(\frac{A_{SH}}{\pi}\right)} \tag{2}$$

$$\varepsilon_{xy} = \frac{\Delta L}{L} = \frac{(R_{OSoil-i} - R_{OSoil})}{(R_{OSoil-i} - R_{ISoil-i})} \tag{3}$$

where: $R_{OSoil\text{-}i}$ is the initial outer radius of the (initially) saturated soil specimen (5.30 cm). Typically, knowledge of soil's shrinkage and swelling properties and knowledge of the range of water contents under consideration would determine whether an independent

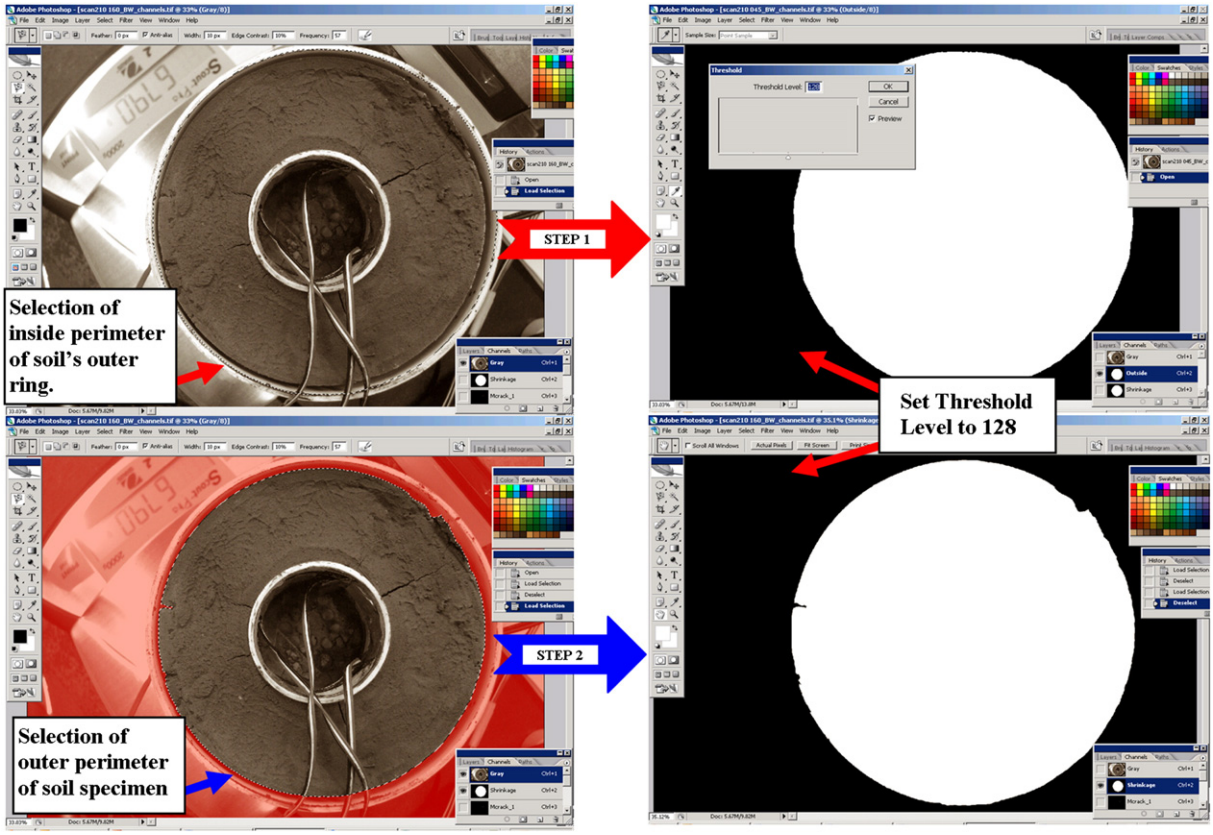

Fig. 2. The procedure for shrinkage calculation using digital image correlation methods: Step 1 involves the selection of the inside perimeter of the outside ring for pixel area calibration and Step 2 involves the selection of the outer perimeter of the soil specimen to calculate the area of the shrinking specimen.

account of vertical shrinkage is required (using either LVDTs or an instrumented caliper). For this study, all the experiments were conducted starting with an initial water content around 36% by mass (around field capacity) and ending at a gravimetric water content in the range of 22–24% (compared to a wilting point around 15–17%). Within this range of gravimetric water contents, the specimen is drier than in the initial shrinkage phase (at saturation) which is dominated by vertical shrinkage (Lura et al., 2007). Thus, an initial extension of this work to (overall) volume change can be achieved by assuming isotropic deformations to approximate shrinkage in the vertical direction from determinations of the (xy) horizontal strain (Eq. (3)). For the range of water contents relevant to this study, this approximation is reasonable, since the soil system is mostly past the air-entry moisture content of around 38% gravimetric (Lura et al., 2007), and thus for the (ring) geometry evaluated, vertical deformations will be proportional to horizontal (xy) deformations.

3. Experimental results and discussion

This section presents experimental results which describe the effects of solution salinity on horizontal deformations as measured using the RRM and digital image correlation method. The results are analyzed and qualitatively interpreted using existing concepts of drying. The authors appreciate that the volumetric response (horizontal and vertical) of the soil system is influenced by a variety of parameters including soil texture, chemistry, mineralogy, clay content and spatial scale. However, for the sake of simplicity and to restrict the complexity of the problem, this paper examines only the effect of the salt concentration on horizontal deformations.

Fig. 3 illustrates (using calculated and previously published datasets) the change in water activity, surface tension, viscosity, and density for solutions containing different amounts of NaCl. It should be noted that some of these relationships are solute dependent. For example, as opposed to NaCl, certain solution properties such as surface tension can follow different trends when other solutes (e.g., KOH) are used (Li and Lu, 2001).

3.1. Rate of drying: experimental observations and correlation to theory

Fig. 4(a) shows the influence of solution salinity on the measured rate of moisture loss from the soil specimen. It is evident that an increase in the salinity of the solution acts to decrease the rate of evaporation. Conceptually, the rate of evaporation (M_{RW}, kg/s.m^2) of a liquid from an exposed surface can be expressed as a function of the difference between the equilibrium vapor pressure of the evaporating liquid and the ambient vapor pressure as shown in Eq. (4) (Kays et al., 2005; Lura et al., 2007):

$$M_{RW} = K(p_L - p_A) \tag{4}$$

where: K is a constant known as the evaporation coefficient that depends on the geometry of the evaporation setup, the properties of the liquid and vapor phase and the flowing air velocity, p_L is the vapor pressure of the evaporating liquid (kPa) and p_A is the ambient vapor pressure (kPa).

Since the vapor pressure of the liquid phase and the ambient air are proportional to the saturation pressure at a specific temperature, p_{sat} (kPa) for a porous medium which contains curved air–liquid menisci, Eq. (4) can be formulated as shown in Eq. (5) (Lura et al., 2003, 2007; Sant et al., 2011):

$$M_{RW} = Kp_{sat}(a_W - RH) = Kp_{sat}a_W(1 - RH_K) \tag{5}$$

where: a_W is the activity of the water component contained in the liquid phase (a value between 0 and 1, fraction) and RH is the equilibrium relative humidity of the environment. Eq. (5) suggests that evaporation will continue so long as $a_W > RH$ and that a reduction in the water activity of the liquid phase would correspondingly reduce the rate of evaporation. In fact, the equilibrium partial vapor pressure of water vapor (i.e., approximated as the relative humidity; RH) includes contributions of: (1) the water activity (a_W) of the solution as described using mixing rules (e.g., Raoult's law), and (2) the curvature (radius) of the interfacial liquid–vapor meniscus (the Kelvin effect; RH_K) through the Kelvin–Laplace equation. Mathematically, this can be generalized as $RH = a_W \cdot (RH_K)$ (Lura et al., 2003 and Sant et al., 2011). For pure, bulk water; $a_W = 1$ and RH_K is equivalent to the equilibrium RH. In the case of salt solutions or water contained in the pore spaces of an unsaturated porous medium; a_W and RH_K have values less than unity. Assuming similar evaporation conditions and soil (pore) structure for the different soil/salt treatments, the contribution of the meniscus (RH_K) is assumed similar and the major change in the bulk response is attributable to the water activity

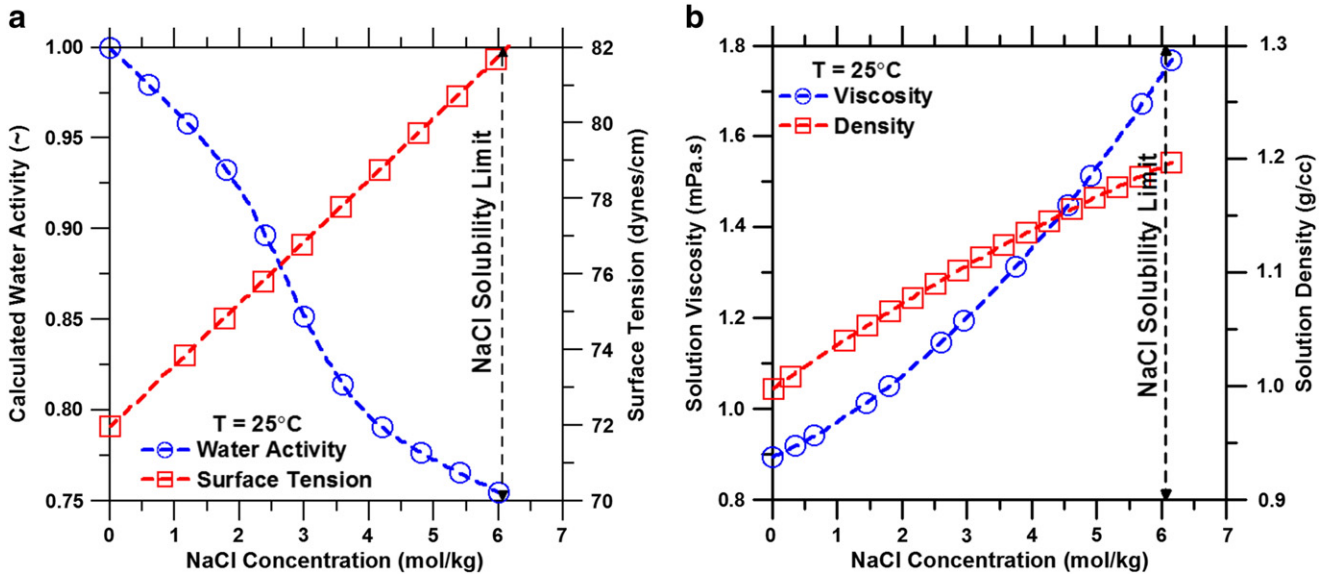

Fig. 3. (a) The calculated water activity and interfacial liquid–vapor surface tension as a function of NaCl concentration (Pruppacher and Klett, 1997). The water activity was calculated using Pitzer's equations (Pitzer, 1979) and (b) the solution viscosity and density as a function of the NaCl concentration (Dougherty, 2001; Kestin et al., 1981).

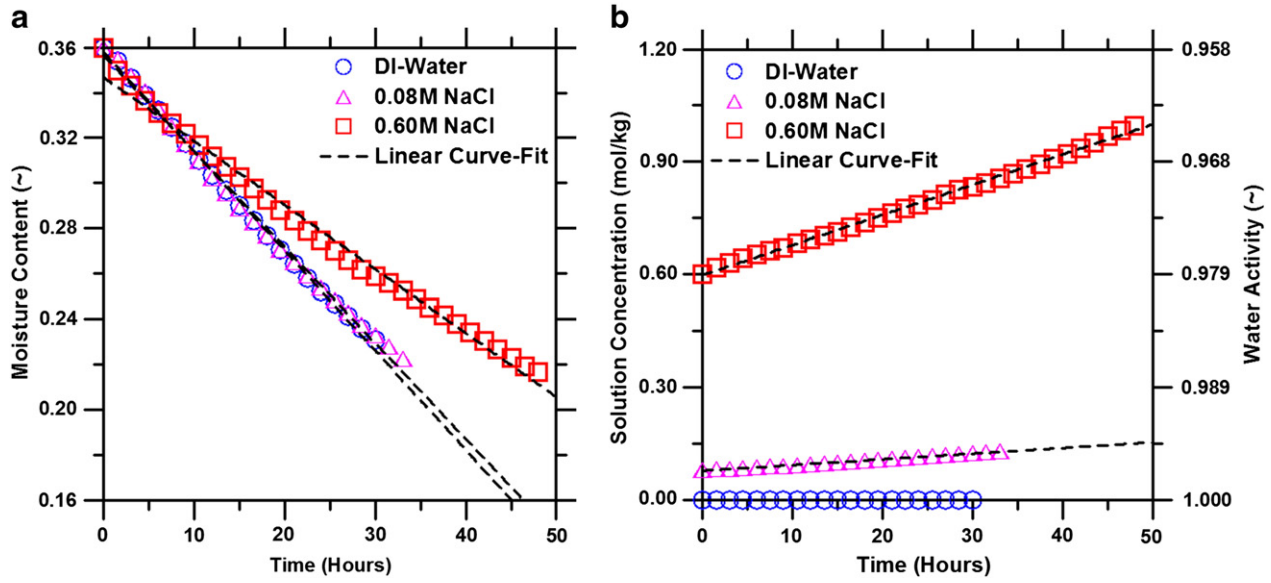

Fig. 4. (a) The decrease in the measured soil moisture content as a function of time due to drying and (b) the change in the NaCl concentration calculated using Eq. (7) and the water activity of the pore solution as a function of drying time. It is noted that the water activity decreases with increasing NaCl concentration.

alteration. The influence of water activity change on the RH_K contribution (and negative pressure) for NaCl systems is shown in Fig. 5.

This explains the experimental results shown in Fig. 4(a) wherein keeping all other parameters (soil structure, environmental conditions) unchanged, a reduction in the water activity due to salt addition would reduce the driving force for evaporation. Obviously, this is an approximation as the soil's structure in swelling soils is in continuous change, as estimated by the shrinkage curve. Finally, the rate of fluid-flow to the evaporation surface can be described using Darcy's law as shown in Eq. (6.a) and (6.b) for saturated and unsaturated soils, respectively (Brinker and Scherer, 1990; Hu et al., 2007; Selker et al., 1999; Sumner, 2000):

$$J_S = \varphi \frac{D}{\eta} \nabla P_S = \varphi \frac{M_{RW}}{\rho} \tag{6.a}$$

$$J_S = \varphi \frac{D}{\eta} \nabla P_S \left(\frac{L}{L_e}\right)^2 \tag{6.b}$$

where: J_S (m/s) is the flux of liquid being transported to the solid surface which is proportional to the rate of evaporation of the liquid from the surface, η is the viscosity of the liquid (Pa.s), D is the intrinsic permeability of the porous medium (m^2), and ∇P_S is the pressure gradient that exists from the interior to the (evaporating) surface of the medium and drives fluid-flow (Pa/m), ϕ is the porosity at the specimen surface from which evaporation can occur, (L_e/L) is the tortuosity; i.e., the ratio of the actual flow length (L_e) to the shortest flow length (L) (Selker et al., 1999; Sumner, 2000), and ρ is the density of the liquid phase (kg/m^3). A finite evaporation rate ensures that liquid flows in the direction of highest pressure; that is from the interior to the surface of the body from where evaporation occurs. Eq. (6) then suggests that an increase of the viscosity and/or the density of the liquid would act to reduce fluid-flow to the evaporation surface. Since the addition of sodium chloride elevates both the viscosity and density of the pore-fluid (Fig. 3), this is another component which ensures saline solutions contained in soil specimens would show slower evaporation than pure water. This, however, becomes more complicated when the soil desaturates (Eq. (6.b)) as aspects related to an increase in the tortuosity of fluid pathways and a reduction in porosity can additionally act to impede fluid movement through the system.

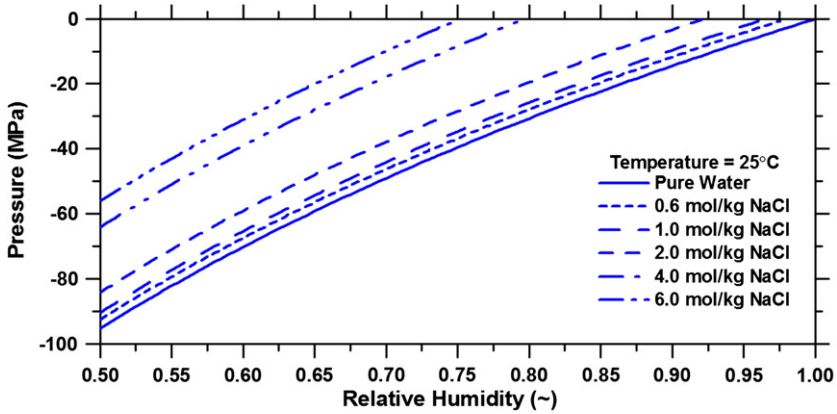

Fig. 5. The influence of the water activity on the negative pressure developed as a function of the ambient equilibrium RH calculated using Equation 9(c). The trend shows that the pressure decreases as the NaCl concentration increases (i.e., the water activity decreases).

Fig. 4(b) shows the increase in the average solution concentration (calculated using Eq. (7)) that occurs as the soil dries and the salt content increases with continuing moisture loss.

$$C(t) = \left(\frac{MC(i)}{MC(t)}\right) C(i) \quad (7)$$

where: C(t) is the calculated (average) concentration (mol/kg) of the solution at time t (hours), MC(i) is the measured initial gravimetric moisture content of the soil specimen (unitless), MC(t) is the measured gravimetric moisture content (unitless) of the soil specimens at any time t (hours) and C(i) is the measured initial concentration of the solution (mol/kg). Though this calculation may suggest a uniform salt concentration (in solution) throughout the specimen, in fact, this is a departure from reality, as the solution is most dilute in the center of the specimen (assuming symmetric drying) and most concentrated at surfaces from where water evaporates — hence being described as an "average concentration". This is important as the concentration gradient that develops acts to ensure the diffusion of ions from the surface of the specimen to the centre and augment the flow of water towards the evaporation surface (Scherer, 1990).

Fig. 4(b) also shows the correspondent decrease in the (calculated, average) water activity (determined from correlation to Fig. 3a) which acts to suppress evaporation in saline solutions. Here it should be noted that the 0.08 M NaCl and DI-water systems show small differences in the evaporation rate, in spite of a difference in the calculated water activity. This can be explained by considering that while the addition of a small quantity of salt does indeed (very slightly) depress the water activity, dominantly, at low salt concentrations soil structure (meniscus, RH_K) effects rather than the water activity control the moisture-loss response. However, the influence of water activity (and solution viscosity, density) is much more clearly noted at higher salt concentrations (0.60 M NaCl) wherein evaporation is clearly reduced. Especially at higher salt contents (0.60 M NaCl) the evaporation curve deviates from linearity, likely due to a progressive (non-linear) decrease in the water activity and increase in the solution viscosity with an increasing (salt) concentration in solution. A possible additional mechanism which produces this response may be the crystallization of salt in pores at the evaporation surface, which may contribute to reducing immediate surface porosity and obstruct water loss (Coussy, 2006; Rodriguez-Navarro and Doenhe, 1999; Scherer, 1999). Each of these aspects is important as the systematic depression produced in the water activity with increasing drying has implications on the driving forces of deformations (negative pressures, Fig. 5) and will be discussed in further detail below.

3.2. Drying stress and strain: experimental observations and correlation to theory

Fig. 6(a) shows the measured internal (drying) stress as a function of time for solutions of different salinities. First, a period of expansion is noted, when a negative (i.e., compressive, expansion driven) stress develops. This likely occurs due to the rearrangement of the soil and the release of consolidation pressures that are applied during specimen preparation. It should be noted that the DIC procedure as implemented can only quantify 2D-horizontal (shrinkage) strains and it cannot quantify any initial (vertical or horizontal) expansions that may occur at the inner or outer boundary of the ring specimen while the soil and rings are in proximate contact. However, as the soil dries, the drying stress overwhelms the expansion stress until a net tensile (i.e., shrinkage driven) internal stress develops as the soil specimen retracts away from the outer ring boundary. This transition occurs at gravimetric moisture contents around 0.31–0.33 (by mass), depending on the salinity of the pore-fluid (Fig. 6b). The delay noted in this transition (Fig. 6a) is caused by the altered properties of saline solutions which ensure retarded evaporation/shrinkage stress development. Critically, the temporal stress-and-strain response indicates that the rate of stress/strain development decreases with increasing salinity, similar to evaporation. In addition, as noted in Fig. 6(b), the drying stress developed at equal moisture contents also appears to slightly decrease with an increasing salt concentration.

Fig. 7 shows the measured 2D-(shrinkage) strain as a function of time and the gravimetric moisture content for soil specimens saturated with solutions of different salinities. On a temporal scale (Fig. 7a), it is noted that as the salinity increases, similar to the drying stress response, the rate of shrinkage decreases. For example, while the DI-water and 0.08 M NaCl specimens show a small difference in shrinkage, the 0.60 M NaCl system shows a considerable increase in the time required to cause equivalent shrinkage. Finally, though to a lesser extent, a similar response is noted for the shrinkage–moisture content (Fig. 7b) relationship wherein the strain developed at equal

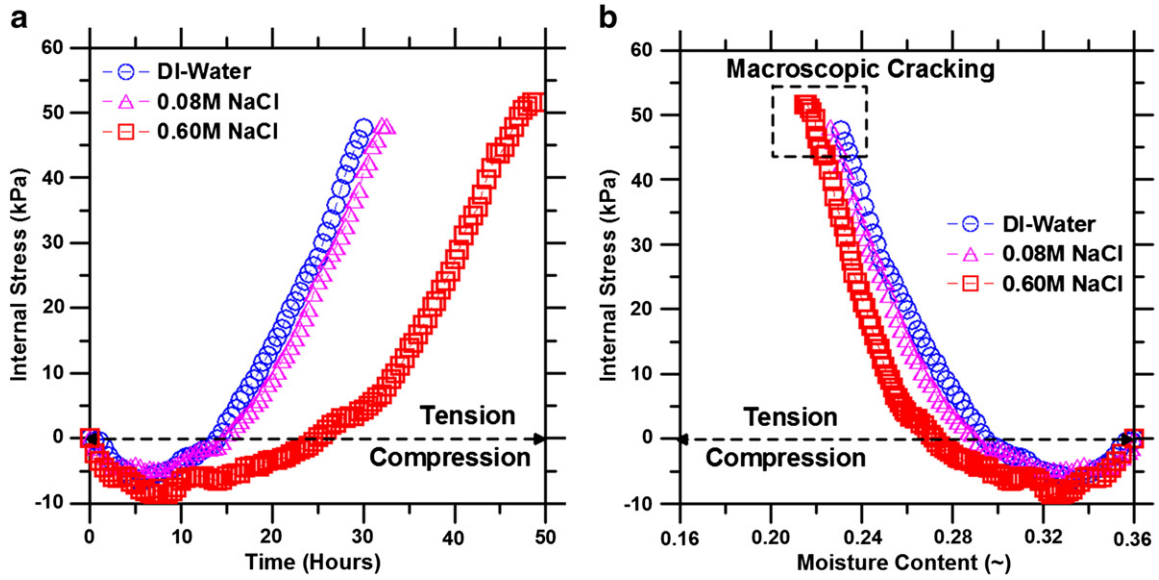

Fig. 6. (a) The measured internal stress developed in the specimen as a function of time caused due to drying and (b) the measured internal stress as a function of the moisture content.

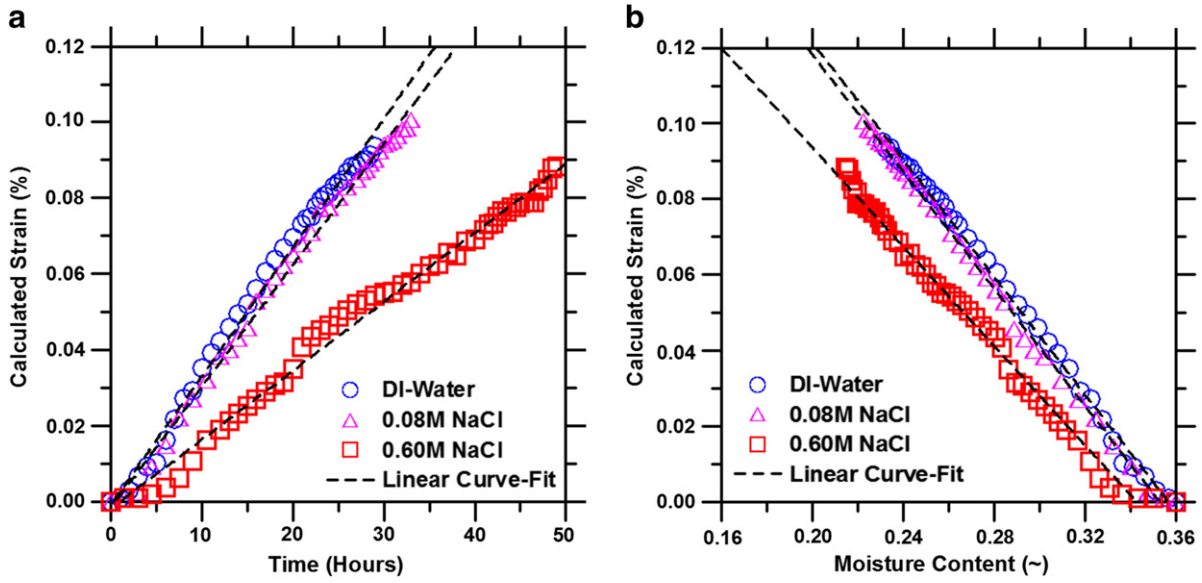

Fig. 7. (a) The measured shrinkage strain as a function of time caused due to drying and (b) the measured strain as a function of the moisture content of the soil specimen. Note that the shrinkage strain is the horizontal, two-dimensional strain measured using DIC. The current procedure did not measure vertical shrinkage independently. Thus the initial expansion detected by the strain gages (Fig. 6) is likely manifested in the vertical direction and was not detected by the DIC technique as applied in this study.

(gravimetric) moisture contents decreases with increasing solution salinity.

The drying stress/strain results are better considered by interrelating the pore solution parameters to stress/strain development during drying. As evaporation progresses from the soil surface, suction forces draw liquid from the interior of the body to the surface to satisfy the evaporation demand. As long as the transport of liquid to the surface is sufficient to satisfy the evaporation demand, air–liquid menisci exist at the surface of the body and only moderate stresses develop. However, when the internal-transport of water is insufficient to satisfy evaporation, liquid–vapor menisci penetrate into the pores at the surface and begin to exert a growing shrinkage stress on the pore walls. In plastic systems, the point at which this occurs is known as the critical point or air-entry value; when the risk of plastic shrinkage cracking is highest (Simpkins et al., 1986, 1989). At the pore-scale, the magnitude of the negative pressure that develops due to moisture loss (drying) in the plastic/hardened state (for frictional/cohesive materials) can be calculated using the Young–Laplace relation as shown in Eq. (8) as a function of the solution's surface tension and the meniscus radius:

$$\frac{P_T = 2\gamma\cos(\theta)}{r_M} \tag{8}$$

where: P_T is the total pressure (when the liquid is in tension, as during drying, this corresponds to negative pressure) that develops (MPa), γ is the liquid–vapor surface tension of the liquid (N/m), θ is the solid–liquid contact angle (assumed to be similar for all systems independent of the salt concentration, degrees) and r_M is the radius of the meniscus that exists at the liquid–vapor interface (negative when the center of curvature is in the vapor phase (Scherer, 1990), m). Conventionally, Eq. (8) describes the capillary pressure that develops as a function of the solution's surface tension and the interfacial meniscus radius. The presence of a solute is expected to alter the surface tension and hence the pressure that develops. Therefore for the sake of clarity and to establish equivalence to Eq. (9), the term total pressure is used. It should be noted that for the case of pure water (unadulterated by a solute) the total pressure (P_T) and the capillary pressure (P_{CAP}) are equivalent.

The capillary pressure developed can also be represented using Kelvin's equation as a function of the relative humidity (RH) of the environment (for specimens at equilibrium with or exposed to the external environment) or the internal relative humidity (for progressively drying specimens) and the correspondent water activity of the solution, as shown in Eq. (9). In each of these cases, the pressure developed is negative, implying that the liquid is in tension and causes a compressive (shrinkage inducing) stress on the pore-walls.

$$P_T = P_{CAP} - P_{OSM} \tag{9a}$$

$$P_T = \frac{\ln(RH)RT}{V_M} - \frac{\ln(a_W)RT}{V_M} \tag{9b}$$

$$P_T = \frac{\ln\left(RH/a_W\right)RT}{V_M} \tag{9c}$$

where: R is the gas constant (8.314 J/K.mol), T is the thermodynamic temperature (298.15 K) and V_M is the molar volume of the liquid phase (assumed to be water; 18.02 cm^3/mol). It should be noted that the total pressure (P_T) developed is a combination of the matric and osmotic suction contributions (Eq. (9)) (Dao et al., 2008; Lura and Lothenbach, 2010; Lura et al., 2003), where the matric component (capillary pressure, P_{CAP}, MPa) is linked to the effects of drying (Kelvin effect), while the osmotic contribution (P_{OSM}, MPa) is a function of the ion concentration of the solution (Raoult effect). First, it is important to indicate that the osmotic pressure is not a pressure in the mechanical sense; rather it is a description of the decrease in the chemical potential of water due to the presence of dissolved salts compared to pure water. Thus, it is a quantification of the potential that would drive osmotic action under conditions of chemical inequilibrium (Robinson and Stokes, 2002). Second, under conditions of partial saturation, as applicable in this study, the effective shrinkage inducing stress acting on the solid (soil) phase is calculated by multiplying the capillary pressure by the degree of fluid saturation to account for the reduced contact area (volume) of solid–liquid surfaces. As such, if the addition of salts acts to maintain a higher degree of fluid saturation (by limiting evaporation) this is a factor which requires consideration in shrinkage stress calculations. However, given the small difference in the degree of saturation (moisture content) in saline and non-saline soils evaluated in this study (Fig. 4a), for the most part, this is a second order effect which can be neglected at a first approximation (Bentz et al., 1998).

A combined examination of Eqs. (8) and (9) describes their relevance in the case of specific boundary conditions to which the specimen is exposed (i.e., sealed or open to the environment). In the case of drying conditions, as were imposed in this study, Eq. (9) is of relevance as it describes the negative pressure as a function of the external RH (to which the specimen is exposed and will eventually equilibrate) and the activity of the pore solution. In this case, it must be noted that until the specimen's moisture level equilibrates with the external environment, the water activity decreases continuously due to drying and the corresponding increase in the (salt) concentration of the pore solution before attaining a static level. Depending on the specific impact of the solute on the pore solution properties, this suggests that: (1) a depression in the surface tension with salt addition (for sealed conditions) and (2) a depression of the water activity with salt addition (for drying conditions) would both reduce the magnitude of the negative pressure (i.e., shrinkage inducing stresses) developed in an unsaturated soil system.

As such, once the total pressure described by Eq. (9c) is known; this can be substituted into Eq. (8) to determine the size of pores that empty for a given value of the solution's surface tension (which changes with the salt concentration). This information suggests that as the solution's surface tension changes (non-linearly with the water activity), the size (radius) of pores that are empty at a given RH level (moisture content) changes accordingly. This is an important point as it indicates that, while Eq. (9) can describe the suction stress developed, Eq. (8) describes the pore structural effect in terms of the size of pores that may be empty or yet remain saturated. For example: at equal RHs and at equilibrium, the size of pores that are empty in a specimen with pure water solution (lower surface tension) is smaller as compared to a specimen with saturated NaCl solution (higher surface tension) as there is lesser resistance to evaporation of a solution which has a lower surface tension. This may indicate a slightly higher fluid saturation level for NaCl containing soils at equal RHs as compared to non-saline soils.

In summary, the above discussion describes the influence of the solution properties on the macroscopic rate and magnitude of the stress/strain response in two ways. First, the reduction in the water activity and the increase in the solution viscosity and density retard evaporation and the rates of stress/strain development. Second, by reducing the water activity and the shrinkage inducing stresses (i.e., negative pressure, Fig. 5), the addition of NaCl ensures that a slightly smaller stress develops in saline systems as compared to non-saline systems at equal moisture contents. A proportionality between stress-and-strain indicates that a reduction in the negative pressure developed by the addition of salts (NaCl) would decrease shrinkage assuming that the mechanical properties remain independent of changes in the salinity level. It should be noted, however, that these inferences assume that the equilibration period of 24 h ensures that salt–clay interactions have already occurred and their effect does not influence the drying response through changes in the elastic properties or prevalent saturation level. However, more research is needed to understand the kinetics of salt–soil structure interaction during drying in more detail.

Moreover, if the bulk modulus of the soil is assumed not to vary considerably with changes in the degree of saturation (i.e., bulk density and porosity vary to a limited extent during volume change (Smith et al., 1995)), it can be inferred that the deformation of the body is controlled by the rate of evaporation of the liquid and the shrinkage stress developed which are directly related to the water activity, viscosity and density of the solution. Overall, it may be expected that soils doped with NaCl (i.e., saline soils) would be expected to shrink less than comparable non-saline soils as the reduction in the shrinkage inducing stress developed due to water activity depression outweighs surface tension effects which act to elevate the fluid saturation level of the porous body (Figs. 6 and 7). On a closing note, while the earlier observation of decreased internal drying stress at equivalent gravimetric moisture contents largely explains the strain-gravimetric moisture content relationship (Fig. 7b), this point may be complicated by the fact that the stiffness of soils has been observed to increase as the salinity level increases (Reeve et al., 1954). While this does explain why more-saline soils fail at a higher internal stress (Fig. 6b), it also suggests that the bulk modulus of the different soil specimens at equivalent gravimetric moisture contents may not be strictly the same. As such, a two-part effect related to: (1) a reduction in the shrinkage inducing stresses (due to water activity effects) and (2) an increase in the stiffness of the soil with increasing solution salinity (and decreasing moisture content) (Towner, 1987) may both act to induce a reduction in stress-and-strain development at equivalent moisture levels (refer to Figs. 6b/7b) in saline soil systems.

3.3. A consideration of parameters that produce experimental variability

Expectedly, great care was taken to ensure uniform sample preparation and conditioning for all the experiments. As indicated earlier, the samples were dried under laboratory conditions ($T = 23 \pm 2$ °C and $RH = 50 \pm 10\%$). This fluctuation in the environmental conditions would, in-turn, induce some variability in the results. To better quantify the impact of experimental conditions on the validity of results, the coefficient of variation (CV; ratio of standard deviation to the mean) was determined for the drying (ring) stress and DIC strain parameters for each 0.5% decrement in the gravimetric water content. Unsurprisingly, a high CV (>1) was observed for strain results at high water contents (the beginning of the experiments) which systematically reduced to a $CV < 0.10$ at a water content around 22% ($CV = 0.02$ for DI-water and $CV = 0.09$ for the high salinity case). Similarly, high CV (>1) was observed for drying stress results at high gravimetric water contents (the beginning of the experiments) which then systematically reduced to $CV < 0.15$ at a water content around 22% ($CV = 0.04$ for DI-water and $CV = 0.15$ for the high salinity case). This quantification demonstrates that slight variations in experimental conditions and material heterogeneity do induce some variability in the results when the sample is wet and the consolidation pressure is being progressively released. However, a statistical treatment of the datasets performed at later time scales (though performed for a limited dataset) does support the validity of the results and the experimental approach of assessment (Dixon, 1986). In light of this argument, the experimental results presented represent (valid) median values of stress-and-strain plotted against moisture content/drying time as applicable to the NaCl treatment (Dixon, 1986).

4. Summary and conclusions

This paper investigates the influence of pore solution properties on the horizontal deformation response of soil systems at the laboratory scale. Restrained ring and DIC-based sensing methods are used to quantify and describe drying stress/strain evolution in unsaturated soils. The results are interpreted while explicitly considering the impact of the pore solution concentration and properties on the stress/strain developed during drying.

The results indicate that the solution concentration (salinity) directly influences a range of parameters ranging from the evaporation and shrinkage rate, to the internal stress that develops at specific gravimetric moisture contents. By increasing the NaCl concentration of the pore-fluids, the rate of evaporation, shrinkage and drying stress development are all decreased. Moreover, the shrinkage and internal stress developed at equivalent gravimetric moisture contents is also decreased. This outcome conforms within interpretations of traditional drying theories and their correlation to the reduction in the water activity and increase in the surface tension, viscosity and density produced by the addition of NaCl to the pore-fluid. Broadly, and in conjunction with each other, the alteration of the solution

properties ensures a reduced evaporation rate and also acts to decrease the shrinkage stress (and strain) developed in the soil.

An important extension to this work would be studying the effect of salinity on soil structure. This is a fundamental component for the extension of the results of this work to the field-scale, particularly as it relates to cracking. While this work suggests that soils containing a high amount of salts may need longer drying periods to crack and may be able to remain uncracked (as compared to non-saline soils) when drying periods are short, the complexity of the soil behavior at the field-scale, structural changes and other processes will influence the overall shrinkage and cracking behavior.

Acknowledgements

The authors would like to acknowledge Dr. Chiara "Clarissa" Ferraris of the National Institute of Standards and Technology (NIST) for providing the particle size distribution of the Chalmers Silty-Clay Loam as measured using laser diffraction methods. The authors would also like to acknowledge the Multi-scale Hydrology Laboratory at the Department of Agricultural and Biological Engineering of Purdue University for conducting the DIC and RRM experiments. This research is based on work partially supported by the National Science Foundation under Grant Number: 0943682 and the USDA under Grant number: 2005–03338.

References

Abou Najm, M., Mohtar, R.H., Weiss, J., Braudeau, E., 2009. Assessing internal stress evolution in unsaturated soils. Water Resources Research 45, W00C11. http://dx.doi.org/10.1029/2007WR006484.

Abou Najm, M. R. (2009), Soil water interaction: Lessons across scales, Ph.D. dissertation, Purdue Univ., West Lafayette, Indiana.

Abou Najm, M., Jabro, J.D., Iversen, W.M., Mohtar, R.H., Evans, R.G., 2010. New method for the characterization of three-dimensional preferential flow paths in the field. Water Resources Research 46, W02503. http://dx.doi.org/10.1029/2009WR008594.

Baumgartl, T., Koeck, B., 2004. Modeling volume change and mechanical properties with hydraulic models. Soil Science Society of America Journal 68, 57–65.

Bentz, D., Garboczi, E.J., Quenard, D.A., 1998. Modeling drying shrinkage in reconstructed porous materials: application to porous Vycor glass. Modeling and Simulation in Materials Science and Engineering 6, 211–236.

Brinker, C.J., Scherer, G.W., 1990. Sol–gel Science. Academic Press, New York, pp. 407–513.

Bogner, C., Wolf, B., Schlather, M., Huwe, B., 2008. Analysing flow patterns from dye tracer experiments in a forest soil using extreme value statistics. European Journal of Soil Science 59 (1), 103–113.

Braudeau, E., Frangi, J., Mohtar, R., 2004. Characterizing nonrigid dual porosity structured soil medium using its shrinkage curve. Soil Science Society of America Journal 68, 359–370.

Braudeau, E., Mohtar, R.H., 2006. Modelling the swelling curve for packed soil aggregates using the pedostructure concept. Soil Science Society of America Journal 70, 494–502.

Chertkov, V.Y., 2007. The reference shrinkage curve at higher than critical soil clay content. Soil Science Society of America Journal 71 (3), 641–655.

Chertkov, V.Y., 2008a. Using the reference shrinkage curve to estimate the corrected crack volume of a soil layer. The Open Mechanics Journal 2, 21–27.

Chertkov, V.Y., 2008b. The physical effects of an intra-aggregate structure on soil shrinkage. Geoderma 146, 147–156.

Chertkov, V.Y., 2010. Two-factor model of soil suction from capillarity, shrinkage, adsorbed film, and intra-aggregate structure. The Open Hydrology Journal 4, 44–64.

Cornelis, W., Corluy, J., Medina, H., Diaz, J., Hartmann, R., van Meirvenne, M., Ruiz, M., 2006. Measuring and modeling the soil shrinkage characteristic curve. Geoderma 137, 179–191.

Coussy, O., Eymard, R., Lassabatère, T., 1998. Constitutive modeling of unsaturated drying deformable materials. Journal of Engineering Mechanics 124 (6), 658–667.

Coussy, O., 2006. Deformation and stress from in-pore drying induced crystallization of salt. Journal of the Mechanics and Physics of Solids 54 (8), 1517–1547.

Dao, V.N.T., Morris, P.H., Dux, P.F., 2008. On equations for the total suction and its matric and osmotic components. Cement and Concrete Research 38, 1302–1305.

Dane, J., Klute, A., 1977. Salt effects on the hydraulic properties of a swelling soil. Soil Science Society of America Journal 41, 1043–1049.

Delage, P., 2007. Microstructure Features in the Behaviour of Engineered Barriers for Nuclear Waste Disposal. In: Schanz, T. (Ed.), Experimental unsaturated soil mechanics. Springer, pp. 11–32.

Dixon, W., et al., 1986. Extraneous Values, In: Klute, A. (Ed.), Methods of soil analysis. Part 1, 2nd ed. : Agron. Monogr., No. 9. ASA and SSSA, Madison, WI, pp. 83–90.

Fityus, S., Buzzi, O., 2009. The place of expansive clays in the framework of unsaturated soil mechanics. Applied Clay Science 43, 150–155.

Dougherty, R.C., 2001. Density of salt solutions. The Journal of Physical Chemistry. B 105, 4514–4519.

Fredlund, D., Morgenstern, M., 1977. Stress State Variables for Unsaturated Soils. Journal of the Geotechnical Engineering Division 103 (5), 447–466.

Fredlund, D., Rahardjo, H., 1993. Soil Mechanics for unsaturated soils. John Wiley & Sons, Inc, New York. Pages, p. 517.

Giraldez, J., Sposito, G., Delgado, C., 1983. A general soil volume change equation: I. The two parameter model. Soil Science Society of America Journal 47, 419–422.

Giraldez, J., Sposito, G., 1983. A general soil volume change equation: II. Effect of load pressure. Soil Science Society of America Journal 47, 422–425.

Hossain, A., Weiss, W., 2004. Assessing residual stress development and stress relaxation in restrained concrete ring specimens. Journal of Cement and Concrete Composites 26, 531–540.

Hu, L.B., Person, H., Hueckel, T., Laloui, L., 2007. Drying shrinkage of deformable porous media: mechanisms induced by fluid removal, ASCE Geo-Denver 2007: New Peaks in Geotechnics, GSP 157: Computer Applications in Geotechnical Engineering, pp. 1–10.

Jozefaciuk, G., Toth, T., Szendrei, G., 2006. Surface and micropore properties of saline soil profiles. Geoderma 135, 1–15.

Kays, W.M., Crawford, M.E., Weigand, B., 2005. Convective Heat and Mass Transfer, 4th edition. McGraw Hill, Boston, Mass. 512 pp.

Kestin, J., Ezzat Khalifa, H., Correia, R.J., 1981. Tables of the dynamics and kinematics viscosity of aqueous NaCl solutions in the temperature range 20–150 Celsius and the pressure range 0.1–35 MPa. Journal of Physical Chemistry 10 (1), 71–87.

Khalili, N., Geiser, F., Blight, G., 2004. Effective stress in unsaturated soils: review with new evidence. International Journal of Geomechanics 4 (2), 115–126.

Kung, K.J.S., Kladivko, E.J., Gish, T.J., Steenhuis, T.S., Bubenzer, G., Helling, C.S., 2000. Quantifying preferential flow by breakthrough of sequentially applied tracers: silt loam soil. Soil Science Society of America Journal 64 (4), 1296–1304.

Li, Z., Lu, B., 2001. Surface tension of aqueous electrolyte solutions at high concentrations — representation and prediction. Chemical Engineering Science 56, 2879–2888.

Lima, L., Grismer, M., 1992. Soil crack morphology and soil salinity. Soil Science 153 (2), 149–153.

Lura, P., Jensen, O.M., van Breugel, K., 2003. Autogenous shrinkage in high-performance cement paste: an evaluation of basic mechanisms. Cement and Concrete Research 33 (2), 223–232.

Lura, P., Pease, B., Mazzotta, G.B., Rajabipour, F., Weiss, W.J., 2007. Influence of shrinkage-reducing admixtures on development of plastic shrinkage cracks. ACI Materials Journal 104 (2), 187–194.

Lura, P., Lothenbach, B., 2010. Influence of pore solution chemistry on shrinkage of cement paste. In: Miao, C., Ye, G., Chen, H. (Eds.), RILEM Proceedings Pro071: Advances in Civil Engineering Materials, pp. 191–200.

Matyas, E., Radhakrishna, H., 1968. Volume change characteristics of partially saturated soil. Geotechnique 18, 432–448.

McGarry, D., Malafant, K.W.J., 1987. The analysis of volume change in unconfined units of soil. Soil Science Society of America Journal 51, 290–297.

McNeal, B., Norvell, W., Coleman, N., 1966. Effect of solution composition on the swelling of extracted soil clays. Soil Science Society of America Journal 30, 313–317.

Murray, E., 2002. An equation of state for unsaturated soils. Can. J. Geotech. 39, 125–140.

Musielak, G., Mierzwa, D., 2009. Permanent strains in clay-like material during drying. Drying Technology 27, 894–902.

Olsen, P., Haugen, L., 1998. A new model of shrinkage characteristic applied to some Norwegian soils. Geoderma 83, 67–81.

Or, D., Tuller, M., 1999. Liquid retention and interfacial area in variably saturated porous media: upscaling from single-pore to sample-scale model. Water Resources Research 35 (12), 3591–3605.

Oster, J., Schroer, F., 1979. Infiltration as influenced by irrigation water quality. Soil Science Society of America Journal 43, 444–447.

Peng, X., Horn, R., Peth, S., Smucker, A., 2006. Quantification of soil shrinkage in 2D by digital image processing of soil surface. Soil Tillage & Research 91, 173–180.

Péron, H., Hu, L., Hueckel, T., Laloui, L., 2007. The influence of the pore fluid on desiccation of a deformable porous material. In: Schanz, T. (Ed.), Experimental unsaturated soil mechanics, Springer, pp. 413–420.

Pitzer, K.S., 1979. Theory—ion interaction approach. In: Pytkowicz, R.M. (Ed.), Activity Coefficients in Electrolyte Solutions, v. 1. CRC Press, Inc, Boca Raton, Florida.

Pruppacher, H.R., Klett, J.D., 1997. Microphysics of Clouds and Precipitation, second edition. Kluwer Academic Publishers, Dordrecht, The Netherlands. 954 pp.

Reeve, R., Bower, C., Brooks, R., Gschwend, F., 1954. A comparison of the effects of exchangeable sodium and potassium upon the physical condition of soils. Soil Science Society of America Journal 18, 130–132.

Robinson, R.A., Stokes, R.H., 2002. Electrolyte Solutions, 2nd ed. Dover, Mineola, N. Y. 571 pp.

Rodriguez-Navarro, C., Doenhe, E., 1999. Salt weathering: influence of evaporation rate, supersaturation and crystallization pattern. Earth Surface Processes and Landforms 24 (3), 191–209.

Roper, H., 1966. Dimensional change and water sorption studies of cement paste. Symposium on Structure of Portland Cement Paste and Concrete. Washington, D.C. pp. 74–83.

Sant, G., Lothenbach, B., Juilland, P., LeSaout, G., Scrivener, K., Weiss, W.J., 2011. The Origin of Early-Age Expansions in Cementitious Materials Containing Shrinkage Reducing Admixtures (SRAs)'. Cement and Concrete Research. doi:10.1016/j.cemconres.2010.12.004.

Sartori, G., Ferrari, A., Pagliai, M., 1985. Changes in soil porosity and surface shrinkage in a remodeled, saline clay soil treated with compost. Soil Science 139 (6), 523–530.

Scherer, G.W., 1990. Theory of Drying. Journal of the American Ceramic Society 73 (1), 3–14.
Scherer, G.W., 1999. Crystallization in pores. Cement and Concrete Research 29 (8), 1347–1358.
Selker, J.S., Keller, G.K., McCord, J.T., 1999. Vadose Zone Processes. CRC Press LLC, Boca Raton, Florida.
Simpkins, P.G., Johnson, D.W., Fleming, D.A., 1986. Drying behavior of colloidal silica gels. Journal of the American Ceramic Society 72 (10), 1816–1821.
Simpkins, P., Johnson, D., Fleming, D., 1989. Drying behavior of colloidal silica gels. Journal of the American Ceramic Society 72 (10), 1816–1821.
Smith, D.M., Scherer, G.W., Anderson, J.M., 1995. Shrinkage during drying of silica gel. Journal of Non-Crystalline Solids 188, 191–206.
Sumner, E.M., 2000. Handbook of soil science. CRC Press, New York, NY.
Taboada, M., Barbosa, O., Cosentino, D., 2008. Null creation of air-filled structural pores by soil cracking and shrinking in silty loamy soils. Soil Science 173 (2), 130–142.
Towner, G.D., 1987. The mechanics of cracking of drying clay. Journal of Agricultural Engineering Research 36, 115–124.
van Genuchten, M., Leij, F., Yates, S., 1991. The RETC code for quantifying the hydraulic functions of unsaturated soils. USDA, US Salinity Laboratory, Riverside, CA. USEPA, EPA/600/2-91/065.
Waller, P., Wallender, W., 1993. Changes in cracking, water content, and bulk density of salinized swelling clay field soils. Soil Science 156 (6), 414–423.
Williams, A.G., Dowd, J.F., Scholefield, D., Holden, N.M., Deeks, L.K., 2003. Preferential flow variability in a well-structured soil. Soil Science Society of America Journal 67 (4), 1272–1281.